



University of
Zurich^{UZH}

Zurich Open Repository and
Archive

University of Zurich
University Library
Strickhofstrasse 39
CH-8057 Zurich
www.zora.uzh.ch

Year: 2019

Observation of $B_{(s)}^0 \rightarrow J/\psi p \bar{p}$ decays and precision measurements of the $B_{(s)}^0$ masses

LHCb Collaboration ; Bernet, Roland ; Müller, Katharina ; Owen, Patrick ; Serra, Nicola ; Steinkamp, Olaf ; Vollhardt, Achim ; et al

DOI: <https://doi.org/10.1103/PhysRevLett.122.191804>

Posted at the Zurich Open Repository and Archive, University of Zurich

ZORA URL: <https://doi.org/10.5167/uzh-180416>

Journal Article

Published Version



The following work is licensed under a Creative Commons: Attribution 4.0 International (CC BY 4.0) License.

Originally published at:

LHCb Collaboration; Bernet, Roland; Müller, Katharina; Owen, Patrick; Serra, Nicola; Steinkamp, Olaf; Vollhardt, Achim; et al (2019). Observation of $B_{(s)}^0 \rightarrow J/\psi p \bar{p}$ decays and precision measurements of the $B_{(s)}^0$ masses. Physical Review Letters, 122(19):191804.

DOI: <https://doi.org/10.1103/PhysRevLett.122.191804>

Observation of $B_{(s)}^0 \rightarrow J/\psi p \bar{p}$ Decays and Precision Measurements of the $B_{(s)}^0$ Masses

R. Aaij *et al.*^{*}
(LHCb Collaboration)

 (Received 18 February 2019; revised manuscript received 26 March 2019; published 17 May 2019)

The first observation of the decays $B_{(s)}^0 \rightarrow J/\psi p \bar{p}$ is reported, using proton-proton collision data corresponding to an integrated luminosity of 5.2 fb^{-1} , collected with the LHCb detector. These decays are suppressed due to limited available phase space, as well as due to Okubo-Zweig-Iizuka or Cabibbo suppression. The measured branching fractions are $\mathcal{B}(B^0 \rightarrow J/\psi p \bar{p}) = [4.51 \pm 0.40(\text{stat}) \pm 0.44(\text{syst})] \times 10^{-7}$, $\mathcal{B}(B_s^0 \rightarrow J/\psi p \bar{p}) = [3.58 \pm 0.19(\text{stat}) \pm 0.39(\text{syst})] \times 10^{-6}$. For the B_s^0 meson, the result is much higher than the expected value of $\mathcal{O}(10^{-9})$. The small available phase space in these decays also allows for the most precise single measurement of both the B^0 mass as $5279.74 \pm 0.30(\text{stat}) \pm 0.10(\text{syst}) \text{ MeV}$ and the B_s^0 mass as $5366.85 \pm 0.19(\text{stat}) \pm 0.13(\text{syst}) \text{ MeV}$.

DOI: 10.1103/PhysRevLett.122.191804

Multiquark hadronic states beyond the well-studied quark-antiquark (meson) and three-quark (baryon) combinations remain elusive even 60 years after their prediction in the quark model [1,2]. Employing an amplitude analysis of $\Lambda_b \rightarrow J/\psi p K^-$ decays, the LHCb collaboration has found states consistent with $|uudc\bar{c}\rangle$ pentaquarks decaying to $J/\psi p$ [3,4] (charge conjugation is implied throughout this Letter). The decays $B_{(s)}^0 \rightarrow J/\psi p \bar{p}$ are sensitive to pentaquark searches in the $J/\psi p$ and $J/\psi \bar{p}$ components and to glueball states [5,6] in the $p \bar{p}$ system. Baryonic $B_{(s)}^0$ decays are also interesting to study the dynamics of the final baryon-antibaryon system and its characteristic threshold enhancement, whose underlying origin has still to be completely understood [7].

In the leading Feynman diagrams shown in Fig. 1, the B^0 mode is Cabibbo suppressed due to the presence of the Cabibbo-Kobayashi-Maskawa element V_{cd} , while the B_s^0 mode is Okubo-Zweig-Iizuka suppressed [2,8,9]. The naïve theoretical expectation for the branching fraction $\mathcal{B}(B_s^0 \rightarrow J/\psi p \bar{p})$ is at the level of 10^{-9} [10]. However, the presence of an intermediate pentaquark or glueball state can enhance the decay rate. The authors of Ref. [10] pointed out the potential sensitivity of $B_s^0 \rightarrow J/\psi p \bar{p}$ decays to tensor glueball states via a possible resonant contribution of $f_J(2220) \rightarrow p \bar{p}$, which could enhance the $B_s^0 \rightarrow J/\psi p \bar{p}$ decay branching fraction up to order 10^{-6} . Hints towards such enhancements were noted in a previous LHCb measurement using 1 fb^{-1} of pp collision data, where

no observation for either mode was made, but a 2.8 standard deviation excess was seen for the $B_s^0 \rightarrow J/\psi p \bar{p}$ decay [11].

These decays also allow for high-precision mass measurements. The kinetic energies in the $B_{(s)}^0$ rest systems of the decay products (Q values) are approximately 306 MeV for B^0 and 393 MeV for B_s^0 decays. The small Q values imply a very small contribution from momentum uncertainties to the $B_{(s)}^0$ mass measurements.

In this Letter, the first observation of these modes along with their branching fraction and B^0 and B_s^0 mass measurements are reported employing a data sample corresponding to 5.2 fb^{-1} of pp collision data collected by the LHCb experiment. As a normalization mode, the copious $B_s^0 \rightarrow J/\psi \phi (\rightarrow K^+ K^-)$ sample is used, which is similar in topology to the signal channels.

The LHCb detector [12,13] is a single-arm forward spectrometer covering the pseudorapidity range $2 < \eta < 5$, designed for the study of particles containing b or c quarks. The detector includes a high-precision tracking system consisting of a silicon-strip vertex detector surrounding the pp interaction region [14], a large-area silicon-strip detector located upstream of a dipole magnet with a bending power of about 4 Tm, and three stations of silicon-strip

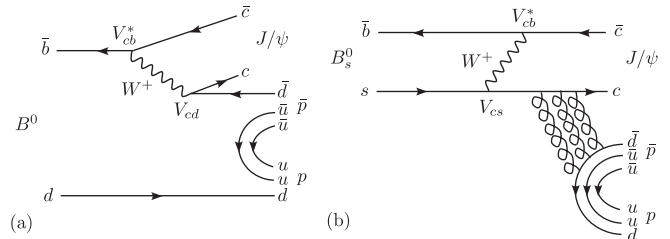


FIG. 1. Leading Feynman diagrams for (a) $B^0 \rightarrow J/\psi p \bar{p}$ and (b) $B_s^0 \rightarrow J/\psi p \bar{p}$ decays.

^{*}Full author list given at end of the article.

Published by the American Physical Society under the terms of the [Creative Commons Attribution 4.0 International license](#). Further distribution of this work must maintain attribution to the author(s) and the published article's title, journal citation, and DOI. Funded by SCOAP³.

detectors and straw drift tubes [15] placed downstream of the magnet. The tracking system provides a measurement of the momentum p of charged particles with a relative uncertainty that varies from 0.5% at low momentum to 1.0% at 200 GeV [16]. Different types of charged hadrons are distinguished using information from two ring-imaging Cherenkov detectors [17]. Muons are identified by a system composed of alternating layers of iron and multiwire proportional chambers [18]. The online event selection is performed by a trigger [19], comprising a hardware stage based on information from the muon system, followed by a software stage that applies a full event reconstruction. The software trigger is a combination of event categories mostly relying on identifying J/ψ decays consistent with a B meson decay topology with two muon tracks originating from a secondary decay vertex detached from the primary pp collision point.

The pp collision data used in this analysis were collected at center-of-mass energies of 7 and 8 TeV (3 fb^{-1}) and 13 TeV (2.2 fb^{-1}), during the run 1 (2011 and 2012) and run 2 (2015 and 2016) run periods, respectively. The data taking conditions differ enough between the two run periods that they are analyzed separately and the results combined at the end.

Samples of simulated events are used to study the properties of the signal and control channels. The pp collisions are generated using PYTHIA [20] with a specific LHCb configuration [21]. Decays of hadronic particles are described by EVTGEN [22], in which final-state radiation is generated using PHOTOS [23]. For the $B_s^0 \rightarrow J/\psi\phi$ mode, simulation samples are generated according to a decay model based on results reported in Ref. [24], while the $B_{(s)}^0 \rightarrow J/\psi p\bar{p}$ signal modes are generated uniformly in phase space. The interactions of the generated particles with the detector and its response are implemented using the GEANT4 toolkit [25] as described in Ref. [26].

The event selection relies on the excellent vertexing and charged particle identification (PID) capabilities of the LHCb detector. For a given particle, the associated primary vertex (PV) corresponds to that with the smallest χ_{IP}^2 , defined as the difference in χ^2 between the PV fit including and excluding the particle. Signal candidates are formed starting with a pair of charged tracks, consistent with muons originating from a common vertex, significantly displaced from its associated PV and with an invariant mass consistent with the J/ψ meson. Another pair of oppositely charged tracks, identified as protons and originating from a common vertex, is combined with the J/ψ candidate to form a $B_{(s)}^0$ candidate. The entire decay topology is submitted to a kinematic fit where the dimuon invariant mass is constrained to the known J/ψ mass [27]. The $B_s^0 \rightarrow J/\psi\phi$ control mode candidates are reconstructed in a similar fashion, replacing the $p\bar{p}$ combination with a pair of charged tracks identified as K^+K^- candidates, required to have an invariant mass within $\pm 5 \text{ MeV}$ of the known ϕ

meson mass [27]. All charged tracks are required to be of good quality and have $p_T > 300 \text{ MeV}$ ($p_T > 550 \text{ MeV}$) for p or K (μ). For the $B_s^0 \rightarrow J/\psi\phi$ mode, the contamination from $B^0 \rightarrow J/\psi K^+\pi^-$ decays with a pion misidentified as a kaon is rejected by imposing a B^0 mass veto and using PID information. At this stage, the combinatorial background dominates, comprising a correctly reconstructed J/ψ meson candidate combined with two unrelated charged tracks.

A multidimensional gradient-boosting (GB) algorithm [28] is used to weight the simulated $B_s^0 \rightarrow J/\psi\phi$ events to match background-subtracted data distributions. This weighting is especially relevant for p and p_T distributions of B mesons. These weights are denoted as GB weights and their distribution has a mean value of one and a standard deviation of 0.38. The background-subtracted data distributions are obtained using the *sPlot* technique [29]. Under the assumption that the relative corrections between data and simulation are similar among different $B_{(s)}^0 \rightarrow J/\psi h^+ h'^-$ decay topologies, h^+ and h'^- being charged hadrons, the GB weights obtained from the control mode are applied to the signal mode. To validate this assumption, similar GB weights are derived using another control mode, $B^0 \rightarrow J/\psi K^+\pi^-$, yielding similar results. For further background suppression, two multivariate classifiers are applied, each employing a gradient-boosted decision tree (BDT) [30]. In the first stage, the BDT_{kin} classifier, based on kinematical and topological variables of the B_s^0 candidate, is trained using the $B_s^0 \rightarrow J/\psi\phi$ decays from simulation as signal proxy and selected $J/\psi p\bar{p}$ candidates in the mass window [5450, 5700] MeV as background. For BDT_{kin} , only kinematic variables whose distributions are similar between the signal and the control mode are employed. These include the p , p_T , and χ_{IP}^2 values of the B_s^0 meson, the χ^2 probability from a kinematic fit [31] to the decay topology, and the impact parameter (IP) of the muons with respect to the associated PV.

To determine the initial signal and background yields, a BDT_{kin} selection requirement is applied to have good signal over background ratio. It is chosen by requiring the $B_s^0 \rightarrow J/\psi p\bar{p}$ signal figure of merit, $S/\sqrt{S+B}$, to exceed five. The background yield B is estimated from a fit to the $J/\psi p\bar{p}$ invariant-mass distribution in a 2σ window around the B_s^0 mass peak, where σ is the invariant-mass resolution. To estimate the expected signal yield S , the central value of the $B_s^0 \rightarrow J/\psi p\bar{p}$ branching fraction quoted in Ref. [11] is used, along with the signal efficiency obtained from simulation.

In the final selection stage, a second classifier, BDT_{PID} , uses the hadron PID information from the Cherenkov detector system to distinguish between pions, kaons, and protons. Aside from PID, the BDT_{PID} training variables also include the p , p_T , and χ_{IP}^2 values of the protons. The signal sample is taken as the $B_s^0 \rightarrow J/\psi p\bar{p}$ simulation incorporating the GB weights for the kinematic variables,

while the background sample is taken from events in data with $m(J/\psi p \bar{p}) \in [5450, 5500]$ MeV. The hadron PID variables in the simulation require further corrections to be representative of data. The PID variables are obtained from high-yield calibration samples of $\Lambda_c^+ \rightarrow p K^- \pi^+$ and $D^{*+} \rightarrow D^0(\rightarrow K^- \pi^+) \pi^+$ decays, which can be selected as a function of the p , p_T , and the number of tracks in the event using only kinematic information [32]. The optimal BDT_{PID} selection criterion is chosen by maximizing the figure of merit $S/\sqrt{S+B}$ with the initial signal and background yields obtained from a fit to the $m(J/\psi p \bar{p})$ distribution after the BDT_{kin} selection.

For the $B_s^0 \rightarrow J/\psi \phi$ control mode, the selection is performed using a dedicated classifier, BDT_{CS} , which includes the kinematic variables considered in BDT_{kin} with the addition of the PID information.

After application of all selection requirements, the background is predominantly combinatorial. Approximately 1% of the selected events contain more than one candidate at this stage; a single candidate is selected randomly. The efficiency of the trigger, detector acceptance, reconstruction, and selection procedure is approximately 1%, as estimated from simulation.

The B^0 and B_s^0 signal and background yields are determined via an extended maximum likelihood fit to the $J/\psi p \bar{p}$ invariant-mass distribution in the range [5220, 5420] MeV. Each signal shape is modeled as the sum of two Crystal Ball [33] functions sharing a common peak position, with tails on either sides of the peak to describe the radiative and misreconstruction effects. The background shape is modeled by a first-order polynomial with parameters determined from the fit to data. The signal-model parameters are determined from simulation and only the B^0 and B_s^0 central mass values are left as free parameters in the fit to data. The detector invariant-mass resolution is in agreement with simulations within a factor of 1.007 ± 0.004 as determined with the control mode. The resolution obtained from simulation is used in the nominal fit and residual discrepancies are accounted for in the systematic uncertainties. In order to validate the fit model, 1000 mass spectra are generated according to the model and fitted employing an alternative model comprising three Gaussian components for the signal and an exponential function for background. The difference between the input value of the yields and the mean of the fitted yields from the alternative model is assigned as a systematic uncertainty. The mass fit for the control mode uses a similar B_s^0 signal line shape, with the background modeled by an exponential function. The result of the fit to the combined run 1 and run 2 control mode yields a signal of 136800 ± 400 . The corresponding fit to the signal-mode candidates is shown in Fig. 2 with the results reported in Table I, where clear signals of B^0 and B_s^0 are observed.

The branching fractions measured with respect to the $B_s^0 \rightarrow J/\psi \phi$ control mode are

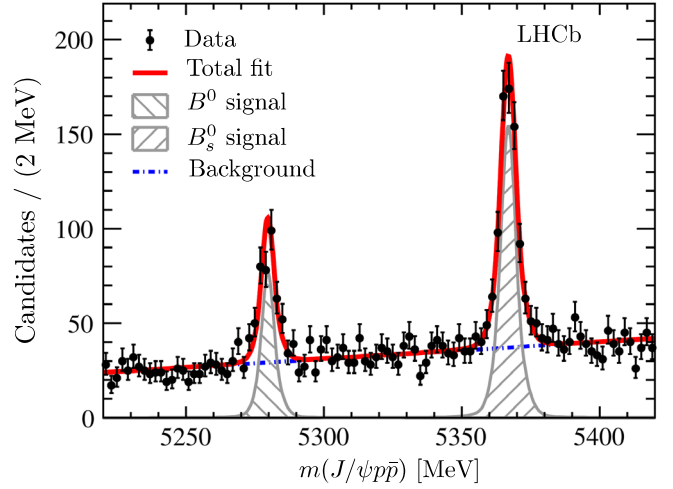


FIG. 2. Fit to the $J/\psi p \bar{p}$ invariant-mass distribution of the $B_{(s)}^0$ signal modes.

$$\frac{\mathcal{B}(B^0 \rightarrow J/\psi p \bar{p})}{\mathcal{B}(B_s^0 \rightarrow J/\psi \phi) \times \mathcal{B}(\phi \rightarrow K^+ K^-) \times f_s/f_d} = \frac{N_{B^0 \rightarrow J/\psi p \bar{p}}^{\text{corr}}}{N_{B_s^0 \rightarrow J/\psi K^+ K^-}^{\text{corr}}},$$

$$\frac{\mathcal{B}(B_s^0 \rightarrow J/\psi p \bar{p})}{\mathcal{B}(B_s^0 \rightarrow J/\psi \phi) \times \mathcal{B}(\phi \rightarrow K^+ K^-)} = \frac{N_{B_s^0 \rightarrow J/\psi p \bar{p}}^{\text{corr}}}{N_{B_s^0 \rightarrow J/\psi K^+ K^-}^{\text{corr}}},$$

where f_s/f_d is the ratio of the b -quark hadronization probabilities into B_s^0 and B^0 mesons, and N^{corr} denotes efficiency-corrected signal yields. For the signal modes, since the physics model is not known *a priori*, an event-by-event efficiency correction is applied to the data. It is derived from simulation as a function of the kinematic variables, which are given in detail in the Supplemental Material [34].

Since the control mode has a topology very similar to that of the signal mode, most of the systematic uncertainties cancel in the branching-fraction ratio measurement. Residual systematic effects of the PID efficiency estimation are due to the correction procedure. An alternative PID correction is considered using proton calibration samples from decays of the long-lived Λ baryon to a proton and a pion, instead of prompt Λ_c^+ decays. The difference between the two methods is assigned as a systematic uncertainty. The degree to which the simulation describes hadronic interactions with the detector material is less accurate for baryons than it is for mesons [22]. Following Ref. [35] a

TABLE I. Signal yields and masses for B^0 and B_s^0 mesons.

Mode	Yield	$B_{(s)}^0$ mass (MeV)
$B^0 \rightarrow J/\psi p \bar{p}$	256 ± 22	5279.74 ± 0.30
$B_s^0 \rightarrow J/\psi p \bar{p}$	609 ± 31	5366.85 ± 0.19

TABLE II. Systematic uncertainties on the branching-fraction measurements for run 1 and run 2. The total uncertainties on the branching-fraction ratios (BFRs) are the sum of the systematic uncertainties, added in quadrature. The total uncertainties on the absolute branching fractions (\mathcal{B}) include the normalization and the uncertainties on the ratio f_s/f_d from external measurements as well.

	$\mathcal{B}(B^0 \rightarrow J/\psi p \bar{p})$	$\mathcal{B}(B_s^0 \rightarrow J/\psi p \bar{p})$
	Run 1 (Run 2)%	Run 1 (Run 2)%
Fit model	1.0 (0.5)	1.0 (0.9)
Detector resolution	0.6 (0.5)	0.4 (0.6)
PID efficiency	5.0 (4.0)	5.0 (4.0)
Trigger	1.0 (1.0)	1.0 (1.0)
Tracking	5.0 (5.0)	5.0 (5.0)
Simulation weighting	0.4 (0.4)	0.3 (0.3)
Multiple candidates	0.1 (0.1)	0.1 (0.1)
Total on BFR	7.2 (6.5)	7.2 (6.6)
Normalization	6.1 (6.1)	6.1 (6.1)
f_s/f_d	-(4.3)	5.8 (5.8)
Total on \mathcal{B}	9.4(10.1)	11.1 (10.7)

systematic uncertainty of 4% (1.1%) per proton (kaon) is assigned for the tracking efficiency of the signal (normalization mode), which is assumed to be fully correlated for the two hadrons with opposite charge. Other systematic effects include the choice of the fit model, weighting procedure, trigger efficiency, and presence of events with more than one candidate. The overall systematic uncertainties on the ratio of branching fractions are 7.2% (7.2%) and 6.5% (6.6%) for B_s^0 (B^0) meson in run 1 and run 2, respectively, where the relevant contributions, listed in Table II, are added in quadrature. Since the detector and the analysis methods remain the same between the two run periods, the systematic uncertainties are fully correlated, while the statistical uncertainties are uncorrelated. The combination of the measurements is taken as a weighted mean to give the branching-fraction ratios

$$\frac{\mathcal{B}(B^0 \rightarrow J/\psi p \bar{p})}{\mathcal{B}(B_s^0 \rightarrow J/\psi \phi) \times \mathcal{B}(\phi \rightarrow K^+ K^-) \times f_s/f_d} = [0.329 \pm 0.029(\text{stat}) \pm 0.022(\text{syst})] \times 10^{-2},$$

$$\frac{\mathcal{B}(B_s^0 \rightarrow J/\psi p \bar{p})}{\mathcal{B}(B_s^0 \rightarrow J/\psi \phi) \times \mathcal{B}(\phi \rightarrow K^+ K^-)} = [0.706 \pm 0.037(\text{stat}) \pm 0.048(\text{syst})] \times 10^{-2},$$

where the first uncertainty is statistical and the second is systematic. For the absolute branching-fraction determination, the value $\mathcal{B}(B_s^0 \rightarrow J/\psi \phi) \times \mathcal{B}(\phi \rightarrow K^+ K^-) \times f_s/f_d = (1.314 \pm 0.016 \pm 0.079) \times 10^{-4}$ is obtained from Ref. [36] as the product of the two branching ratios, $\mathcal{B}(B_s^0 \rightarrow J/\psi \phi) = (10.50 \pm 0.13 \pm 0.64) \times 10^{-4}$ and $\mathcal{B}(\phi \rightarrow K^+ K^-) = 0.489 \pm 0.005$, and the ratio of fragmentation probabilities $f_s/f_d = 0.256 \pm 0.020$ [37]. For the B_s^0 meson normalization, the updated ratio

$f_s/f_d = 0.259 \pm 0.015$ [37] is used in run 1, while for run 2 it has been multiplied by an additional scale factor of 1.068 ± 0.046 [38] to take into account the dependence on the center of mass energy. The small S -wave $K^+ K^-$ fraction under the $\phi(1020)$ resonance, $F_S = 0.0070 \pm 0.0005$ [36], is accounted for as a correction. The absolute branching fractions are then combined to give

$$\mathcal{B}(B^0 \rightarrow J/\psi p \bar{p}) = [4.51 \pm 0.40(\text{stat}) \pm 0.44(\text{syst})] \times 10^{-7},$$

$$\mathcal{B}(B_s^0 \rightarrow J/\psi p \bar{p}) = [3.58 \pm 0.19(\text{stat}) \pm 0.39(\text{syst})] \times 10^{-6},$$

where the systematic uncertainty is the sum in quadrature of the overall systematic contribution on the ratio of branching fractions, the normalization mode uncertainty, and the f_s/f_d uncertainty for the B_s^0 signal. Table II summarizes the systematic uncertainties separately for the run periods. The dominant contributions are the normalization, the PID, and the tracking systematic uncertainties. For the B^0 meson, the external normalization measurement from run 1, $\mathcal{B}(B_s^0 \rightarrow J/\psi \phi) \times \mathcal{B}(\phi \rightarrow K^+ K^-) \times f_s/f_d$ [36], is used, while for run 2 the additional energy-dependent correction on f_s/f_d has an uncertainty of 4.3%. For the B_s^0 meson, the measured $\mathcal{B}(B_s^0 \rightarrow J/\psi \phi) \times \mathcal{B}(\phi \rightarrow K^+ K^-) \times f_s/f_d$ is divided by f_s/f_d to obtain the B_s^0 normalization, $\mathcal{B}(B_s^0 \rightarrow J/\psi \phi) \times \mathcal{B}(\phi \rightarrow K^+ K^-)$, resulting in an uncertainty on f_s/f_d independent of the run condition.

In addition, the small Q values of the $B_{(s)}^0 \rightarrow J/\psi p \bar{p}$ decays also allow for precise measurements of the B^0 and B_s^0 masses, with a resolution of 3.3 MeV (3.8 MeV) for the B^0 (B_s^0) meson. The main systematic uncertainty is related to imperfections in the momentum reconstruction. The momentum scale is calibrated using samples of $J/\psi \rightarrow \mu^+ \mu^-$ and $B^+ \rightarrow J/\psi K^+$ decays collected concurrently with the data sample used for this analysis [39,40]. The relative accuracy of this procedure is estimated to be 3×10^{-4} using samples of other fully reconstructed b hadrons, Υ and K_S^0 mesons. Other systematic effects are due to uncertainties on particle interactions with the detector material and to the choice of the signal model, as reported in Table III. The uncertainty on the J/ψ mass is included in the momentum scaling contribution. The final results are

TABLE III. Systematic uncertainties of B^0 and B_s^0 mass measurements.

	B^0	B_s^0
	(MeV)	(MeV)
Momentum scale	0.097	0.124
Mass fit model	0.020	0.020
Energy loss correction	0.030	0.030
Total	0.103	0.129

$$m_{B^0} = 5279.74 \pm 0.30(\text{stat}) \pm 0.10(\text{syst}) \text{ MeV},$$

$$m_{B_s^0} = 5366.85 \pm 0.19(\text{stat}) \pm 0.13(\text{syst}) \text{ MeV},$$

with a correlation of 4×10^{-4} in the statistical uncertainty. These represent the most precise single measurements for the B^0 and B_s^0 masses.

In summary, the first observation of the $B^0 \rightarrow J/\psi p \bar{p}$ and $B_s^0 \rightarrow J/\psi p \bar{p}$ decays is reported. The measured branching fraction for the $B^0 \rightarrow J/\psi p \bar{p}$ decay is consistent with theoretical expectations [10] while that for $B_s^0 \rightarrow J/\psi p \bar{p}$ is enhanced by 2 orders of magnitude with respect to predictions without resonant contributions [10]. More data are needed for glueball and pentaquark searches through a full Dalitz plot analysis. The world's best single measurements of the B^0 and B_s^0 masses are also reported.

We express our gratitude to our colleagues in the CERN accelerator departments for the excellent performance of the LHC. We thank the technical and administrative staff at the LHCb institutes. We acknowledge support from CERN and from the following national agencies: CAPES, CNPq, FAPERJ, and FINEP (Brazil); MOST and NSFC (China); CNRS/IN2P3 (France); BMBF, DFG, and MPG (Germany); INFN (Italy); NWO (Netherlands); MNiSW and NCN (Poland); MEN/IFA (Romania); MSHE (Russia); MinECo (Spain); SNSF and SER (Switzerland); NASU (Ukraine); STFC (United Kingdom); and NSF (USA). We acknowledge the computing resources that are provided by CERN, IN2P3 (France), KIT and DESY (Germany), INFN (Italy), SURF (Netherlands), PIC (Spain), GridPP (United Kingdom), RRCKI and Yandex LLC (Russia), CSCS (Switzerland), IFIN-HH (Romania), CBPF (Brazil), (France), KIT and DESY (Germany), INFN (Italy), SURF (Netherlands), PIC (Spain), GridPP (United Kingdom), RRCKI and Yandex LLC (Russia), CSCS (Switzerland), IFIN-HH (Romania), CBPF (Brazil), PL-GRID (Poland), and OSC (USA). We are indebted to the communities behind the multiple open-source software packages on which we depend. Individual groups or members have received support from Fondazione Fratelli Confalonieri (Italy), AvH Foundation (Germany); EPLANET, Marie Skłodowska-Curie Actions and ERC (European Union); ANR, Labex P2IO and OCEVU, and Région Auvergne-Rhône-Alpes (France); Key Research Program of Frontier Sciences of CAS, CAS PIFI, and the Thousand Talents Program (China); RFBR, RSF, and Yandex LLC (Russia); GVA, XuntaGal, and GENCAT (Spain); the Royal Society and the Leverhulme Trust (United Kingdom); and Laboratory Directed Research and Development program of LANL (USA).

[1] M. Gell-Mann, *Phys. Lett.* **8**, 214 (1964).

[2] G. Zweig, CERN Technical Report No. CERN-TH-401, 1964.

- [3] R. Aaij *et al.* (LHCb Collaboration), *Phys. Rev. Lett.* **115**, 072001 (2015).
- [4] R. Aaij *et al.* (LHCb Collaboration), *Phys. Rev. Lett.* **117**, 082002 (2016).
- [5] C. J. Morningstar and M. Peardon, *Phys. Rev. D* **60**, 034509 (1999).
- [6] Y. Chen *et al.*, *Phys. Rev. D* **73**, 014516 (2006).
- [7] J. L. Rosner, *Phys. Rev. D* **68**, 014004 (2003).
- [8] S. Okubo, *Phys. Lett.* **5**, 165 (1963).
- [9] J. Iizuka, *Prog. Theor. Phys. Suppl.* **37**, 21 (1966).
- [10] Y. K. Hsiao and C. Q. Geng, *Eur. Phys. J. C* **75**, 101 (2015).
- [11] R. Aaij *et al.* (LHCb Collaboration), *J. High Energy Phys.* **09** (2013) 006.
- [12] A. A. Alves, Jr. *et al.* (LHCb Collaboration), *J. Instrum.* **3**, S08005 (2008).
- [13] R. Aaij *et al.* (LHCb Collaboration), *Int. J. Mod. Phys. A* **30**, 1530022 (2015).
- [14] R. Aaij *et al.*, *J. Instrum.* **9**, P09007 (2014).
- [15] R. Arink *et al.*, *J. Instrum.* **9**, P01002 (2014).
- [16] Natural units with $\hbar = c = 1$ are used throughout.
- [17] M. Adinolfi *et al.*, *Eur. Phys. J. C* **73**, 2431 (2013).
- [18] A. A. Alves, Jr. *et al.*, *J. Instrum.* **8**, P02022 (2013).
- [19] R. Aaij *et al.*, *J. Instrum.* **8**, P04022 (2013).
- [20] T. Sjöstrand, S. Mrenna, and P. Skands, *J. High Energy Phys.* **05** (2006) 026; *Comput. Phys. Commun.* **178**, 852 (2008).
- [21] I. Belyaev *et al.*, *J. Phys. Conf. Ser.* **331**, 032047 (2011).
- [22] D. J. Lange, *Nucl. Instrum. Methods Phys. Res., Sect. A* **462**, 152 (2001).
- [23] P. Golonka and Z. Was, *Eur. Phys. J. C* **45**, 97 (2006).
- [24] R. Aaij *et al.* (LHCb Collaboration), *Phys. Rev. Lett.* **114**, 041801 (2015).
- [25] J. Allison, K. Amako, J. Apostolakis, H. Araujo, P. Dubois *et al.* (GEANT4 Collaboration), *IEEE Trans. Nucl. Sci.* **53**, 270 (2006); S. Agostinelli *et al.* (GEANT4 Collaboration), *Nucl. Instrum. Methods Phys. Res., Sect. A* **506**, 250 (2003).
- [26] M. Clemencic, G. Corti, S. Easo, C. R. Jones, S. Miglioranza, M. Pappagallo, and P. Robbe, *J. Phys. Conf. Ser.* **331**, 032023 (2011).
- [27] M. Tanabashi *et al.* (Particle Data Group), *Phys. Rev. D* **98**, 030001 (2018).
- [28] A. Rogozhnikov, *J. Phys. Conf. Ser.* **762**, 012036 (2016).
- [29] M. Pivk and F. R. Le Diberder, *Nucl. Instrum. Methods Phys. Res., Sect. A* **555**, 356 (2005).
- [30] L. Breiman, J. H. Friedman, R. A. Olshen, and C. J. Stone, *Classification and Regression Trees* (Wadsworth International Group, Belmont, CA, 1984).
- [31] W. D. Hulsbergen, *Nucl. Instrum. Methods Phys. Res., Sect. A* **552**, 566 (2005).
- [32] R. Aaij *et al.*, *EPJ Tech. Instrum.* **6**, 1 (2019).
- [33] T. Skwarnicki, Ph. D. thesis, Institute of Nuclear Physics, Krakow, 1986, DESY-F31-86-02.
- [34] See Supplemental Material at <http://link.aps.org/supplemental/10.1103/PhysRevLett.122.191804> for details on the event-by-event efficiency parametrization and combination procedure of the branching fractions from the two run periods.

- [35] R. Aaij *et al.* (LHCb Collaboration), *J. High Energy Phys.* **04** (2017) 162.
- [36] R. Aaij *et al.* (LHCb Collaboration), *Phys. Rev. D* **87**, 072004 (2013).
- [37] R. Aaij *et al.* (LHCb Collaboration), *J. High Energy Phys.* **04** (2013) 001, f_s/f_d value updated in LHCb-CONF-2013-011.
- [38] R. Aaij *et al.* (LHCb Collaboration), *Phys. Rev. Lett.* **118**, 191801 (2017).
- [39] R. Aaij *et al.* (LHCb Collaboration), *Phys. Rev. Lett.* **110**, 182001 (2013).
- [40] R. Aaij *et al.* (LHCb Collaboration), *J. High Energy Phys.* **06** (2013) 065.

R. Aaij,²⁹ C. Abellán Beteta,⁴⁶ B. Adeva,⁴³ M. Adinolfi,⁵⁰ C. A. Aidala,⁷⁷ Z. Ajaltouni,⁷ S. Akar,⁶¹ P. Albicocco,²⁰ J. Albrecht,¹² F. Alessio,⁴⁴ M. Alexander,⁵⁵ A. Alfonso Alberio,⁴² G. Alkhazov,³⁵ P. Alvarez Cartelle,⁵⁷ A. A. Alves Jr.,⁴³ S. Amato,² S. Amerio,²⁵ Y. Amhis,⁹ L. An,¹⁹ L. Anderlini,¹⁹ G. Andreassi,⁴⁵ M. Andreotti,¹⁸ J. E. Andrews,⁶² F. Archilli,²⁹ J. Arnau Romeu,⁸ A. Artamonov,⁴¹ M. Artuso,⁶³ K. Arzymatov,³⁹ E. Aslanides,⁸ M. Atzeni,⁴⁶ B. Audurier,²⁴ S. Bachmann,¹⁴ J. J. Back,⁵² S. Baker,⁵⁷ V. Balagura,^{9,b} W. Baldini,¹⁸ A. Baranov,³⁹ R. J. Barlow,⁵⁸ G. C. Barrand,⁹ S. Barsuk,⁹ W. Barter,⁵⁸ M. Bartolini,²¹ F. Baryshnikov,⁷³ V. Batzskaya,³³ B. Batsukh,⁶³ A. Battig,¹² V. Battista,⁴⁵ A. Bay,⁴⁵ J. Beddow,⁵⁵ F. Bedeschi,²⁶ I. Bediaga,¹ A. Beiter,⁶³ L. J. Bel,²⁹ S. Belin,²⁴ N. Belyi,⁴ V. Bellec,⁴⁵ N. Belloli,^{22,i} K. Belous,⁴¹ I. Belyaev,³⁶ G. Bencivenni,²⁰ E. Ben-Haim,¹⁰ S. Benson,²⁹ S. Beranek,¹¹ A. Berezhniov,³⁷ R. Bernet,⁴⁶ D. Berninghoff,¹⁴ E. Bertholet,¹⁰ A. Bertolin,²⁵ C. Betancourt,⁴⁶ F. Betti,^{17,44} M. O. Bettler,⁵¹ Ia. Bezshyiko,⁴⁶ S. Bhasin,⁵⁰ J. Bhom,³¹ M. S. Bieker,¹² S. Bifani,⁴⁹ P. Billoir,¹⁰ A. Birnkraut,¹² A. Bizzeti,^{19,u} M. Björn,⁵⁹ M. P. Blago,⁴⁴ T. Blake,⁵² F. Blanc,⁴⁵ S. Blusk,⁶³ D. Bobulska,⁵⁵ V. Bocci,²⁸ O. Boente Garcia,⁴³ T. Boettcher,⁶⁰ A. Bondar,^{40,x} N. Bondar,³⁵ S. Borghi,^{58,44} M. Borisyak,³⁹ M. Borsato,⁴³ M. Boubdir,¹¹ T. J. V. Bowcock,⁵⁶ C. Bozzi,^{18,44} S. Braun,¹⁴ M. Brodski,⁴⁴ J. Brodzicka,³¹ A. Brossa Gonzalo,⁵² D. Brundu,^{24,44} E. Buchanan,⁵⁰ A. Buonauro,⁴⁶ C. Burr,⁵⁸ A. Bursche,²⁴ J. Buytaert,⁴⁴ W. Byczynski,⁴⁴ S. Cadeddu,²⁴ H. Cai,⁶⁷ R. Calabrese,^{18,g} R. Calladine,⁴⁹ M. Calvi,^{22,i} M. Calvo Gomez,^{42,m} A. Camboni,^{42,m} P. Campana,²⁰ D. H. Campora Perez,⁴⁴ L. Capriotti,^{17,e} A. Carbone,^{17,e} G. Carboni,²⁷ R. Cardinale,²¹ A. Cardini,²⁴ P. Carniti,¹⁰ K. Carvalho Akiba,² G. Casse,⁵⁶ M. Cattaneo,⁴⁴ G. Cavallero,²¹ R. Cenci,^{26,p} D. Chamont,⁹ M. G. Chapman,⁵⁰ M. Charles,¹⁰ Ph. Charpentier,⁴⁴ G. Chatzikonstantinidis,⁴⁹ M. Chefdeville,⁶ V. Chekalina,³⁹ C. Chen,³ S. Chen,²⁴ S.-G. Chitic,⁴⁴ V. Chobanova,⁴³ M. Chruszcz,⁴⁴ A. Chubykin,³⁵ P. Ciambone,²⁰ X. Cid Vidal,⁴³ G. Ciezarek,⁴⁴ F. Cindolo,¹⁷ P. E. L. Clarke,⁵⁴ M. Clemencic,⁴⁴ H. V. Cliff,⁵¹ J. Closier,⁴⁴ V. Coco,⁴⁴ J. A. B. Coelho,⁹ J. Cogan,⁸ E. Cogneras,⁷ L. Cojocariu,³⁴ P. Collins,⁴⁴ T. Colombo,⁴⁴ A. Comerma-Montells,¹⁴ A. Contu,²⁴ G. Coombs,⁴⁴ S. Coquereau,⁴² G. Corti,⁴⁴ M. Corvo,^{18,g} C. M. Costa Sobral,⁵² B. Couturier,⁴⁴ G. A. Cowan,⁵⁴ D. C. Craik,⁶⁰ A. Crocombe,⁵² M. Cruz Torres,¹ R. Currie,⁵⁴ F. Da Cunha Marinho,² C. L. Da Silva,⁷⁸ E. Dall'Occo,²⁹ J. Dalseno,^{43,v} C. D'Ambrosio,⁴⁴ A. Danilina,³⁶ P. d'Argent,¹⁴ A. Davis,⁵⁸ O. De Aguiar Francisco,⁴⁴ K. De Bruyn,⁴⁴ S. De Capua,⁵⁸ M. De Cian,⁴⁵ J. M. De Miranda,¹ L. De Paula,² M. De Serio,^{16,d} P. De Simone,²⁰ J. A. de Vries,²⁹ C. T. Dean,⁵⁵ W. Dean,⁷⁷ D. Decamp,⁶ L. Del Buono,¹⁰ B. Delaney,⁵¹ H.-P. Dembinski,¹³ M. Demmer,¹² A. Dendek,³² D. Derkach,⁷⁴ O. Deschamps,⁷ F. Desse,⁹ F. Dettori,⁵⁶ B. Dey,⁶⁸ A. Di Canto,⁴⁴ P. Di Nezza,²⁰ S. Didenko,⁷³ H. Dijkstra,⁴⁴ F. Dordei,²⁴ M. Dorigo,^{44,y} A. C. dos Reis,¹ A. Dosil Suárez,⁴³ L. Douglas,⁵⁵ A. Dovbnya,⁴⁷ K. Dreimanis,⁵⁶ L. Dufour,²⁹ G. Dujany,¹⁰ P. Durante,⁴⁴ J. M. Durham,⁷⁸ D. Dutta,⁵⁸ R. Dzhelezadine,^{41,t} M. Dziewiecki,¹⁴ A. Dziurda,³¹ A. Dzyuba,³⁵ S. Easo,⁵³ U. Egede,⁵⁷ V. Egorychev,³⁶ S. Eidelman,^{40,x} S. Eisenhardt,⁵⁴ U. Eitschberger,¹² R. Ekelhof,¹² L. Eklund,⁵⁵ S. Ely,⁶³ A. Ene,³⁴ S. Escher,¹¹ S. Esen,²⁹ T. Evans,⁶¹ A. Falabella,¹⁷ C. Färber,⁴⁴ N. Farley,⁴⁹ S. Farry,⁵⁶ D. Fazzini,^{22,44,i} M. Féo,⁴⁴ P. Fernandez Declara,⁴⁴ A. Fernandez Prieto,⁴³ F. Ferrari,^{17,e} L. Ferreira Lopes,⁴⁵ F. Ferreira Rodrigues,² M. Ferro-Luzzi,⁴⁴ S. Filippov,³⁸ R. A. Fini,¹⁶ M. Fiorini,^{18,g} M. Firlej,³² C. Fitzpatrick,⁴⁵ T. Fiutowski,³² F. Fleuret,^{9,b} M. Fontana,⁴⁴ F. Fontanelli,^{21,h} R. Forty,⁴⁴ V. Franco Lima,⁵⁶ M. Frank,⁴⁴ C. Frei,⁴⁴ J. Fu,^{23,q} W. Funk,⁴⁴ E. Gabriel,⁵⁴ A. Gallas Torreira,⁴³ D. Galli,^{17,e} S. Gallorini,²⁵ S. Gambetta,⁵⁴ Y. Gan,³ M. Gandelman,² P. Gandini,²³ Y. Gao,³ L. M. Garcia Martin,⁷⁶ J. García Pardiñas,⁴⁶ B. Garcia Plana,⁴³ J. Garra Tico,⁵¹ L. Garrido,⁴² D. Gascon,⁴² C. Gaspar,⁴⁴ L. Gavardi,¹² G. Gazzoni,⁷ D. Gerick,¹⁴ E. Gersabeck,⁵⁸ M. Gersabeck,⁵⁸ T. Gershon,⁵² D. Gerstel,⁸ Ph. Ghez,⁶ V. Gibson,⁵¹ O. G. Girard,⁴⁵ P. Gironella Gironell,⁴² L. Giubega,³⁴ K. Gizdov,⁵⁴ V. V. Gligorov,¹⁰ C. Göbel,⁶⁵ D. Golubkov,³⁶ A. Golutvin,^{57,73} A. Gomes,^{1,a} I. V. Gorelov,³⁷ C. Gotti,^{22,i} E. Govorkova,²⁹ J. P. Grabowski,¹⁴ R. Graciani Diaz,⁴² L. A. Granado Cardoso,⁴⁴ E. Graugés,⁴² E. Graverini,⁴⁶ G. Graziani,¹⁹ A. Grecu,³⁴ R. Greim,²⁹ P. Griffith,²⁴ L. Grillo,⁵⁸ L. Gruber,⁴⁴ B. R. Gruber Cazon,⁵⁹ O. Grünberg,⁷⁰ C. Gu,³ E. Gushchin,³⁸ A. Guth,¹¹ Yu. Guz,^{41,44} T. Gys,⁴⁴ T. Hadavizadeh,⁵⁹ C. Hadjivasiliou,⁷ G. Haefeli,⁴⁵ C. Haen,⁴⁴ S. C. Haines,⁵¹ B. Hamilton,⁶² X. Han,¹⁴ T. H. Hancock,⁵⁹ S. Hansmann-Menzemer,¹⁴ N. Harnew,⁵⁹ T. Harrison,⁵⁶

- C. Hasse,⁴⁴ M. Hatch,⁴⁴ J. He,⁴ M. Hecker,⁵⁷ K. Heinicke,¹² A. Heister,¹² K. Hennessy,⁵⁶ L. Henry,⁷⁶ M. Heß,⁷⁰ J. Heuel,¹¹
 A. Hicheur,⁶⁴ R. Hidalgo Charman,⁵⁸ D. Hill,⁵⁹ M. Hilton,⁵⁸ P. H. Hopchev,⁴⁵ J. Hu,¹⁴ W. Hu,⁶⁸ W. Huang,⁴ Z. C. Huard,⁶¹
 W. Hulsbergen,²⁹ T. Humair,⁵⁷ M. Hushchyn,⁷⁴ D. Hutchcroft,⁵⁶ D. Hynds,²⁹ P. Ibis,¹² M. Idzik,³² P. Ilten,⁴⁹ A. Inglessi,³⁵
 A. Inyakin,⁴¹ K. Ivshin,³⁵ R. Jacobsson,⁴⁴ J. Jalocha,⁵⁹ E. Jans,²⁹ B. K. Jashal,⁷⁶ A. Jawahery,⁶² F. Jiang,³ M. John,⁵⁹
 D. Johnson,⁴⁴ C. R. Jones,⁵¹ C. Joram,⁴⁴ B. Jost,⁴⁴ N. Jurik,⁵⁹ S. Kandybei,⁴⁷ M. Karacson,⁴⁴ J. M. Kariuki,⁵⁰ S. Karodia,⁵⁵
 N. Kazeev,⁷⁴ M. Kecke,¹⁴ F. Keizer,⁵¹ M. Kelsey,⁶³ M. Kenzie,⁵¹ T. Ketel,³⁰ E. Khairullin,³⁹ B. Khanji,⁴⁴
 C. Khurewathanakul,⁴⁵ K. E. Kim,⁶³ T. Kim,¹¹ V. S. Kirsabom,⁴⁵ S. Klaver,²⁰ K. Klimaszewski,³³ T. Klimovich,¹³
 S. Koliiev,⁴⁸ M. Kolpin,¹⁴ R. Kopecna,¹⁴ P. Koppenburg,²⁹ I. Kostiuk,^{29,48} S. Kotriakhova,³⁵ M. Kozeiha,⁷ L. Kravchuk,³⁸
 M. Kreps,⁵² F. Kress,⁵⁷ P. Krokovny,^{40,x} W. Krupa,³² W. Krzemien,³³ W. Kucewicz,^{31,1} M. Kucharczyk,³¹ V. Kudryavtsev,^{40,x}
 A. K. Kuonen,⁴⁵ T. Kvaratskheliya,^{36,44} D. Lacarrere,⁴⁴ G. Lafferty,⁵⁸ A. Lai,²⁴ D. Lancierini,⁴⁶ G. Lanfranchi,²⁰
 C. Langenbruch,¹¹ T. Latham,⁵² C. Lazzeroni,⁴⁹ R. Le Gac,⁸ R. Lefèvre,⁷ A. Leflat,³⁷ F. Lemaitre,⁴⁴ O. Leroy,⁸ T. Lesiak,³¹
 B. Leverington,¹⁴ P.-R. Li,^{4,ab} Y. Li,⁵ Z. Li,⁶³ X. Liang,⁶³ T. Likhomanenko,⁷² R. Lindner,⁴⁴ F. Lionetto,⁴⁶ V. Lisovskyi,⁹
 G. Liu,⁶⁶ X. Liu,³ D. Loh,⁵² A. Loi,²⁴ I. Longstaff,⁵⁵ J. H. Lopes,² G. H. Lovell,⁵¹ D. Lucchesi,^{25,o} M. Lucio Martinez,⁴³
 Y. Luo,³ A. Lupato,²⁵ E. Luppi,^{18,g} O. Lupton,⁴⁴ A. Lusiani,²⁶ X. Lyu,⁴ F. Machefert,⁹ F. Maciuc,³⁴ V. Macko,⁴⁵
 P. Mackowiak,¹² S. Maddrell-Mander,⁵⁰ O. Maev,^{35,44} K. Maguire,⁵⁸ D. Maisuzenko,³⁵ M. W. Majewski,³² S. Malde,⁵⁹
 B. Malecki,⁴⁴ A. Malinin,⁷² T. Maltsev,^{40,x} H. Malygina,¹⁴ G. Manca,^{24,f} G. Mancinelli,⁸ D. Marangotto,^{23,q} J. Maratas,^{7,w}
 J. F. Marchand,⁶ U. Marconi,¹⁷ C. Marin Benito,⁹ M. Marinangeli,⁴⁵ P. Marino,⁴⁵ J. Marks,¹⁴ P. J. Marshall,⁵⁶
 G. Martellotti,²⁸ M. Martinelli,⁴⁴ D. Martinez Santos,⁴³ F. Martinez Vidal,⁷⁶ A. Massafferri,¹ M. Materok,¹¹ R. Matev,⁴⁴
 A. Mathad,⁵² Z. Mathe,⁴⁴ C. Matteuzzi,²² A. Mauri,⁴⁶ E. Maurice,^{9,b} B. Maurin,⁴⁵ M. McCann,^{57,44} A. McNab,⁵⁸
 R. McNulty,¹⁵ J. V. Mead,⁵⁶ B. Meadows,⁶¹ C. Meaux,⁸ N. Meinert,⁷⁰ D. Melnychuk,³³ M. Merk,²⁹ A. Merli,^{23,q}
 E. Michielin,²⁵ D. A. Milanes,⁶⁹ E. Millard,⁵² M.-N. Minard,⁶ L. Minzoni,^{18,g} D. S. Mitzel,¹⁴ A. Mödden,¹² A. Mogini,¹⁰
 R. D. Moise,⁵⁷ T. Mombächer,¹² I. A. Monroy,⁶⁹ S. Monteil,⁷ M. Morandin,²⁵ G. Morello,²⁰ M. J. Morello,^{26,t}
 O. Morgunova,⁷² J. Moron,³² A. B. Morris,⁸ R. Mountain,⁶³ F. Muheim,⁵⁴ M. Mukherjee,⁶⁸ M. Mulder,²⁹ D. Müller,⁴⁴
 J. Müller,¹² K. Müller,⁴⁶ V. Müller,¹² C. H. Murphy,⁵⁹ D. Murray,⁵⁸ P. Naik,⁵⁰ T. Nakada,⁴⁵ R. Nandakumar,⁵³ A. Nandi,⁵⁹
 T. Nanut,⁴⁵ I. Nasteva,² M. Needham,⁵⁴ N. Neri,^{23,q} S. Neubert,¹⁴ N. Neufeld,⁴⁴ R. Newcombe,⁵⁷ T. D. Nguyen,⁴⁵
 C. Nguyen-Mau,^{45,n} S. Nieswand,¹¹ R. Niet,¹² N. Nikitin,³⁷ A. Nogay,⁷² N. S. Nolte,⁴⁴ A. Oblakowska-Mucha,³²
 V. Obraztsov,⁴¹ S. Ogilvy,⁵⁵ D. P. O'Hanlon,¹⁷ R. Oldeman,^{24,f} C. J. G. Onderwater,⁷¹ A. Ossowska,³¹
 J. M. Otalora Goicochea,² T. Ovsianikova,³⁶ P. Owen,⁴⁶ A. Oyanguren,⁷⁶ P. R. Pais,⁴⁵ T. Pajero,^{26,t} A. Palano,¹⁶
 M. Palutan,²⁰ G. Panshin,⁷⁵ A. Papanestis,⁵³ M. Pappagallo,⁵⁴ L. L. Pappalardo,^{18,g} W. Parker,⁶² C. Parkes,^{58,44}
 G. Passaleva,^{19,44} A. Pastore,¹⁶ M. Patel,⁵⁷ C. Patrignani,^{17,e} A. Pearce,⁴⁴ A. Pellegrino,²⁹ G. Penso,²⁸ M. Pepe Altarelli,⁴⁴
 S. Perazzini,⁴⁴ D. Pereima,³⁶ P. Perret,⁷ L. Pescatore,⁴⁵ K. Petridis,⁵⁰ A. Petrolini,^{21,h} A. Petrov,⁷² S. Petrucci,⁵⁴
 M. Petruzzo,^{23,q} B. Pietrzyk,⁶ G. Pietrzyk,⁴⁵ M. Pikies,³¹ M. Pili,⁵⁹ D. Pinci,²⁸ J. Pinzino,⁴⁴ F. Pisani,⁴⁴ A. Piucci,¹⁴
 V. Placinta,³⁴ S. Playfer,⁵⁴ J. Plews,⁴⁹ M. Plo Casasus,⁴³ F. Polci,¹⁰ M. Poli Lener,²⁰ A. Poluektov,⁸ N. Polukhina,^{73,c}
 I. Polyakov,⁶³ E. Polcarpo,² G. J. Pomery,⁵⁰ S. Ponce,⁴⁴ A. Popov,⁴¹ D. Popov,^{49,13} S. Poslavskii,⁴¹ E. Price,⁵⁰
 J. Prisciandaro,⁴³ C. Prouve,⁴³ V. Pugatch,⁴⁸ A. Puig Navarro,⁴⁶ H. Pullen,⁵⁹ G. Punzi,^{26,p} W. Qian,⁴ J. Qin,⁴ R. Quagliani,¹⁰
 B. Quintana,⁷ N. V. Raab,¹⁵ B. Rachwal,³² J. H. Rademacker,⁵⁰ M. Rama,²⁶ M. Ramos Pernas,⁴³ M. S. Rangel,²
 F. Ratnikov,^{39,74} G. Raven,³⁰ M. Ravonel Salzgeber,⁴⁴ M. Reboud,⁶ F. Redi,⁴⁵ S. Reichert,¹² F. Reiss,¹⁰ C. Remon Alepuz,⁷⁶
 Z. Ren,³ V. Renaudin,⁵⁹ S. Ricciardi,⁵³ S. Richards,⁵⁰ K. Rinnert,⁵⁶ P. Robbe,⁹ A. Robert,¹⁰ A. B. Rodrigues,⁴⁵
 E. Rodrigues,⁶¹ J. A. Rodriguez Lopez,⁶⁹ M. Roehrken,⁴⁴ S. Roiser,⁴⁴ A. Rollings,⁵⁹ V. Romanovskiy,⁴¹ A. Romero Vidal,⁴³
 J. D. Roth,⁷⁷ M. Rotondo,²⁰ M. S. Rudolph,⁶³ T. Ruf,⁴⁴ J. Ruiz Vidal,⁷⁶ J. J. Saborido Silva,⁴³ N. Sagidova,³⁵ B. Saitta,^{24,f}
 V. Salustino Guimaraes,⁶⁵ C. Sanchez Gras,²⁹ C. Sanchez Mayordomo,⁷⁶ B. Sanmartin Sedes,⁴³ R. Santacesaria,²⁸
 C. Santamarina Rios,⁴³ M. Santimaria,^{20,44} E. Santovetti,^{27,j} G. Sarpis,⁵⁸ A. Sarti,^{20,k} C. Satriano,^{28,s} A. Satta,²⁷ M. Saur,⁴
 D. Savrina,^{36,37} S. Schael,¹¹ M. Schellenberg,¹² M. Schiller,⁵⁵ H. Schindler,⁴⁴ M. Schmelling,¹³ T. Schmelzer,¹²
 B. Schmidt,⁴⁴ O. Schneider,⁴⁵ A. Schopper,⁴⁴ H. F. Schreiner,⁶¹ M. Schubiger,⁴⁵ S. Schulte,⁴⁵ M. H. Schune,⁹
 R. Schwemmer,⁴⁴ B. Sciascia,²⁰ A. Sciubba,^{28,k} A. Semennikov,³⁶ E. S. Sepulveda,¹⁰ A. Sergi,⁴⁹ N. Serra,⁴⁶ J. Serrano,⁸
 L. Sestini,²⁵ A. Seuthe,¹² P. Seyfert,⁴⁴ M. Shapkin,⁴¹ Y. Shcheglov,^{35,†} T. Shears,⁵⁶ L. Shekhtman,^{40,x} V. Shevchenko,⁷²
 E. Shmanin,⁷³ B. G. Siddi,¹⁸ R. Silva Coutinho,⁴⁶ L. Silva de Oliveira,² G. Simi,^{25,o} S. Simone,^{16,d} I. Skiba,¹⁸ N. Skidmore,¹⁴
 T. Skwarnicki,⁶³ M. W. Slater,⁴⁹ J. G. Smeaton,⁵¹ E. Smith,¹¹ I. T. Smith,⁵⁴ M. Smith,⁵⁷ M. Soares,¹⁷ I. Soares Lavra,¹
 M. D. Sokoloff,⁶¹ F. J. P. Soler,⁵⁵ B. Souza De Paula,² B. Spaan,¹² E. Spadaro Norella,^{23,q} P. Spradlin,⁵⁵ F. Stagni,⁴⁴

M. Stahl,¹⁴ S. Stahl,⁴⁴ P. Stefko,⁴⁵ S. Stefkova,⁵⁷ O. Steinkamp,⁴⁶ S. Stemmler,¹⁴ O. Stenyakin,⁴¹ M. Stepanova,³⁵ H. Stevens,¹² A. Stocchi,⁹ S. Stone,⁶³ B. Storaci,⁴⁶ S. Stracka,²⁶ M. E. Stramaglia,⁴⁵ M. Straticiu,³⁴ U. Straumann,⁴⁶ S. Strokov,⁷⁵ J. Sun,³ L. Sun,⁶⁷ Y. Sun,⁶² K. Swientek,³² A. Szabelski,³³ T. Szumlak,³² M. Szymanski,⁴ Z. Tang,³ T. Tekampe,¹² G. Tellarini,¹⁸ F. Teubert,⁴⁴ E. Thomas,⁴⁴ M. J. Tilley,⁵⁷ V. Tisserand,⁷ S. T'Jampens,⁶ M. Tobin,³² S. Tolks,⁴⁴ L. Tomassetti,^{18,g} D. Tonelli,²⁶ D. Y. Tou,¹⁰ R. Tourinho Jadallah Aoude,¹ E. Tournefier,⁶ M. Traill,⁵⁵ M. T. Tran,⁴⁵ A. Trisovic,⁵¹ A. Tsaregorodtsev,⁸ G. Tuci,^{26,p} A. Tully,⁵¹ N. Tuning,^{29,44} A. Ukleja,³³ A. Usachov,⁹ A. Ustyuzhanin,^{39,74} U. Uwer,¹⁴ A. Vagner,⁷⁵ V. Vagnoni,¹⁷ A. Valassi,⁴⁴ S. Valat,⁴⁴ G. Valenti,¹⁷ M. van Beuzekom,²⁹ E. van Herwijnen,⁴⁴ J. van Tilburg,²⁹ M. van Veghel,²⁹ R. Vazquez Gomez,⁴⁴ P. Vazquez Regueiro,⁴³ C. Vázquez Sierra,²⁹ S. Vecchi,¹⁸ J. J. Velthuis,⁵⁰ M. Veltri,^{19,r} G. Veneziano,⁵⁹ A. Venkateswaran,⁶³ M. Vernet,⁷ M. Veronesi,²⁹ M. Vesterinen,⁵² J. V. Viana Barbosa,⁴⁴ D. Vieira,⁴ M. Vieites Diaz,⁴³ H. Viemann,⁷⁰ X. Vilasis-Cardona,^{42,m} A. Vitkovskiy,²⁹ M. Vitti,⁵¹ V. Volkov,³⁷ A. Vollhardt,⁴⁶ D. Vom Bruch,¹⁰ B. Voneki,⁴⁴ A. Vorobyev,³⁵ V. Vorobyev,^{40,x} N. Voropaev,³⁵ R. Waldi,⁷⁰ J. Walsh,²⁶ J. Wang,⁵ M. Wang,³ Y. Wang,⁶⁸ Z. Wang,⁴⁶ D. R. Ward,⁵¹ H. M. Wark,⁵⁶ N. K. Watson,⁴⁹ D. Websdale,⁵⁷ A. Weiden,⁴⁶ C. Weissner,⁶⁰ M. Whitehead,¹¹ G. Wilkinson,⁵⁹ M. Wilkinson,⁶³ I. Williams,⁵¹ M. Williams,⁶⁰ M. R. J. Williams,⁵⁸ T. Williams,⁴⁹ F. F. Wilson,⁵³ M. Winn,⁹ W. Wislicki,³³ M. Witek,³¹ G. Wormser,⁹ S. A. Wotton,⁵¹ K. Wyllie,⁴⁴ D. Xiao,⁶⁸ Y. Xie,⁶⁸ A. Xu,³ M. Xu,⁶⁸ Q. Xu,⁴ Z. Xu,⁶ Z. Xu,³ Z. Yang,³ Z. Yang,⁶² Y. Yao,⁶³ L. E. Yeomans,⁵⁶ H. Yin,⁶⁸ J. Yu,^{68,aa} X. Yuan,⁶³ O. Yushchenko,⁴¹ K. A. Zarebski,⁴⁹ M. Zavertyaev,^{13,c} D. Zhang,⁶⁸ L. Zhang,³ W. C. Zhang,^{3,z} Y. Zhang,⁴⁴ A. Zhelezov,¹⁴ Y. Zheng,⁴ X. Zhu,³ V. Zhukov,^{11,37} J. B. Zonneveld,⁵⁴ and S. Zucchelli^{17,e}

(LHCb Collaboration)

¹*Centro Brasileiro de Pesquisas Físicas (CBPF), Rio de Janeiro, Brazil*

²*Universidade Federal do Rio de Janeiro (UFRJ), Rio de Janeiro, Brazil*

³*Center for High Energy Physics, Tsinghua University, Beijing, China*

⁴*University of Chinese Academy of Sciences, Beijing, China*

⁵*Institute of High Energy Physics (ihep), Beijing, China*

⁶*Université Grenoble Alpes, Université Savoie Mont Blanc, CNRS, IN2P3-LAPP, Annecy, France*

⁷*Université Clermont Auvergne, CNRS/IN2P3, LPC, Clermont-Ferrand, France*

⁸*Aix Marseille Université, CNRS/IN2P3, CPPM, Marseille, France*

⁹*LAL, Université Paris-Sud, CNRS/IN2P3, Université Paris-Saclay, Orsay, France*

¹⁰*LPNHE, Sorbonne Université, Paris Diderot Sorbonne Paris Cité, CNRS/IN2P3, Paris, France*

¹¹*I. Physikalisches Institut, RWTH Aachen University, Aachen, Germany*

¹²*Fakultät Physik, Technische Universität Dortmund, Dortmund, Germany*

¹³*Max-Planck-Institut für Kernphysik (MPIK), Heidelberg, Germany*

¹⁴*Physikalisches Institut, Ruprecht-Karls-Universität Heidelberg, Heidelberg, Germany*

¹⁵*School of Physics, University College Dublin, Dublin, Ireland*

¹⁶*INFN Sezione di Bari, Bari, Italy*

¹⁷*INFN Sezione di Bologna, Bologna, Italy*

¹⁸*INFN Sezione di Ferrara, Ferrara, Italy*

¹⁹*INFN Sezione di Firenze, Firenze, Italy*

²⁰*INFN Laboratori Nazionali di Frascati, Frascati, Italy*

²¹*INFN Sezione di Genova, Genova, Italy*

²²*INFN Sezione di Milano-Bicocca, Milano, Italy*

²³*INFN Sezione di Milano, Milano, Italy*

²⁴*INFN Sezione di Cagliari, Monserrato, Italy*

²⁵*INFN Sezione di Padova, Padova, Italy*

²⁶*INFN Sezione di Pisa, Pisa, Italy*

²⁷*INFN Sezione di Roma Tor Vergata, Roma, Italy*

²⁸*INFN Sezione di Roma La Sapienza, Roma, Italy*

²⁹*Nikhef National Institute for Subatomic Physics, Amsterdam, Netherlands*

³⁰*Nikhef National Institute for Subatomic Physics and VU University Amsterdam, Amsterdam, Netherlands*

³¹*Henryk Niewodniczanski Institute of Nuclear Physics Polish Academy of Sciences, Kraków, Poland*

³²*AGH—University of Science and Technology, Faculty of Physics and Applied Computer Science, Kraków, Poland*

³³*National Center for Nuclear Research (NCBJ), Warsaw, Poland*

³⁴*Horia Hulubei National Institute of Physics and Nuclear Engineering, Bucharest-Magurele, Romania*

³⁵*Petersburg Nuclear Physics Institute (PNPI), Gatchina, Russia*

- ³⁶*Institute of Theoretical and Experimental Physics (ITEP), Moscow, Russia*
- ³⁷*Institute of Nuclear Physics, Moscow State University (SINP MSU), Moscow, Russia*
- ³⁸*Institute for Nuclear Research of the Russian Academy of Sciences (INR RAS), Moscow, Russia*
- ³⁹*Yandex School of Data Analysis, Moscow, Russia*
- ⁴⁰*Budker Institute of Nuclear Physics (SB RAS), Novosibirsk, Russia*
- ⁴¹*Institute for High Energy Physics (IHEP), Protvino, Russia*
- ⁴²*ICCUB, Universitat de Barcelona, Barcelona, Spain*
- ⁴³*Instituto Galego de Física de Altas Enerxías (IGFAE), Universidade de Santiago de Compostela, Santiago de Compostela, Spain*
- ⁴⁴*European Organization for Nuclear Research (CERN), Geneva, Switzerland*
- ⁴⁵*Institute of Physics, Ecole Polytechnique Fédérale de Lausanne (EPFL), Lausanne, Switzerland*
- ⁴⁶*Physik-Institut, Universität Zürich, Zürich, Switzerland*
- ⁴⁷*NSC Kharkiv Institute of Physics and Technology (NSC KIPT), Kharkiv, Ukraine*
- ⁴⁸*Institute for Nuclear Research of the National Academy of Sciences (KINR), Kyiv, Ukraine*
- ⁴⁹*University of Birmingham, Birmingham, United Kingdom*
- ⁵⁰*H.H. Wills Physics Laboratory, University of Bristol, Bristol, United Kingdom*
- ⁵¹*Cavendish Laboratory, University of Cambridge, Cambridge, United Kingdom*
- ⁵²*Department of Physics, University of Warwick, Coventry, United Kingdom*
- ⁵³*STFC Rutherford Appleton Laboratory, Didcot, United Kingdom*
- ⁵⁴*School of Physics and Astronomy, University of Edinburgh, Edinburgh, United Kingdom*
- ⁵⁵*School of Physics and Astronomy, University of Glasgow, Glasgow, United Kingdom*
- ⁵⁶*Oliver Lodge Laboratory, University of Liverpool, Liverpool, United Kingdom*
- ⁵⁷*Imperial College London, London, United Kingdom*
- ⁵⁸*School of Physics and Astronomy, University of Manchester, Manchester, United Kingdom*
- ⁵⁹*Department of Physics, University of Oxford, Oxford, United Kingdom*
- ⁶⁰*Massachusetts Institute of Technology, Cambridge, Massachusetts, USA*
- ⁶¹*University of Cincinnati, Cincinnati, Ohio, USA*
- ⁶²*University of Maryland, College Park, Maryland, USA*
- ⁶³*Syracuse University, Syracuse, New York, USA*
- ⁶⁴*Laboratory of Mathematical and Subatomic Physics, Constantine, Algeria*
[associated with Universidade Federal do Rio de Janeiro (UFRJ), Rio de Janeiro, Brazil]
- ⁶⁵*Pontificia Universidade Católica do Rio de Janeiro (PUC-Rio), Rio de Janeiro, Brazil*
[associated with Universidade Federal do Rio de Janeiro (UFRJ), Rio de Janeiro, Brazil]
- ⁶⁶*South China Normal University, Guangzhou, China*
(associated with Center for High Energy Physics, Tsinghua University, Beijing, China)
- ⁶⁷*School of Physics and Technology, Wuhan University, Wuhan, China*
(associated with Center for High Energy Physics, Tsinghua University, Beijing, China)
- ⁶⁸*Institute of Particle Physics, Central China Normal University, Wuhan, Hubei, China*
(associated with Center for High Energy Physics, Tsinghua University, Beijing, China)
- ⁶⁹*Departamento de Física, Universidad Nacional de Colombia, Bogota, Colombia*
(associated with LPNHE, Sorbonne Université, Paris Diderot Sorbonne Paris Cité, CNRS/IN2P3, Paris, France)
- ⁷⁰*Institut für Physik, Universität Rostock, Rostock, Germany*
(associated with Physikalisches Institut, Ruprecht-Karls-Universität Heidelberg, Heidelberg, Germany)
- ⁷¹*Van Swinderen Institute, University of Groningen, Groningen, Netherlands*
(associated with Nikhef National Institute for Subatomic Physics, Amsterdam, Netherlands)
- ⁷²*National Research Centre Kurchatov Institute, Moscow, Russia*
[associated with Institute of Theoretical and Experimental Physics (ITEP), Moscow, Russia]
- ⁷³*National University of Science and Technology “MISIS,” Moscow, Russia*
[associated with Institute of Theoretical and Experimental Physics (ITEP), Moscow, Russia]
- ⁷⁴*National Research University Higher School of Economics, Moscow, Russia*
(associated with Yandex School of Data Analysis, Moscow, Russia)
- ⁷⁵*National Research Tomsk Polytechnic University, Tomsk, Russia*
[associated with Institute of Theoretical and Experimental Physics (ITEP), Moscow, Russia]
- ⁷⁶*Instituto de Física Corpuscular, Centro Mixto Universidad de Valencia—CSIC, Valencia, Spain*
(associated with ICCUB, Universitat de Barcelona, Barcelona, Spain)
- ⁷⁷*University of Michigan, Ann Arbor, Michigan, USA*
(associated with Syracuse University, Syracuse, New York, USA)
- ⁷⁸*Los Alamos National Laboratory (LANL), Los Alamos, New Mexico, USA*
(associated with Syracuse University, Syracuse, New York, USA)

[†]Deceased.

^aUniversidade Federal do Triângulo Mineiro (UFTM), Uberaba-MG, Brazil.

^bLaboratoire Leprince-Ringuet, Palaiseau, France.

^cP.N. Lebedev Physical Institute, Russian Academy of Science (LPI RAS), Moscow, Russia.

^dUniversità di Bari, Bari, Italy.

^eUniversità di Bologna, Bologna, Italy.

^fUniversità di Cagliari, Cagliari, Italy.

^gUniversità di Ferrara, Ferrara, Italy.

^hUniversità di Genova, Genova, Italy.

ⁱUniversità di Milano Bicocca, Milano, Italy.

^jUniversità di Roma Tor Vergata, Roma, Italy.

^kUniversità di Roma La Sapienza, Roma, Italy.

^lAGH—University of Science and Technology, Faculty of Computer Science, Electronics and Telecommunications, Kraków, Poland.

^mLIFAEELS, La Salle, Universitat Ramon Llull, Barcelona, Spain.

ⁿHanoi University of Science, Hanoi, Vietnam.

^oUniversità di Padova, Padova, Italy.

^pUniversità di Pisa, Pisa, Italy.

^qUniversità degli Studi di Milano, Milano, Italy.

^rUniversità di Urbino, Urbino, Italy.

^sUniversità della Basilicata, Potenza, Italy.

^tScuola Normale Superiore, Pisa, Italy.

^uUniversità di Modena e Reggio Emilia, Modena, Italy.

^vH.H. Wills Physics Laboratory, University of Bristol, Bristol, United Kingdom.

^wMSU—Iligan Institute of Technology (MSU-IIT), Iligan, Philippines.

^xNovosibirsk State University, Novosibirsk, Russia.

^ySezione INFN di Trieste, Trieste, Italy.

^zSchool of Physics and Information Technology, Shaanxi Normal University (SNNU), Xi'an, China.

^{aa}Physics and Micro Electronic College, Hunan University, Changsha City, China.

^{ab}Lanzhou University, Lanzhou, China.